Energy 290 (2024) 130120

Contents lists available at ScienceDirect

Energy

journal homepage: www.elsevier.com/locate/energy

Power flow traceable P2P electricity market segmentation and cost allocation ☆

Chengwei Lou [a], Jin Yang [b,*], Eduardo Vega Fuentes [c], Yue Zhou [d], Liang Min [b], James Yu [e], Nand Kishor Meena [f]

[a] College of Information and Electrical Engineering, China Agricultural University, Beijing, 100083, China
[b] James Watt School of Engineering, University of Glasgow, Glasgow, G12 8QQ, United Kingdom
[c] Institute for Applied Microelectronics, Department of Electrical Engineering, University of Las Palmas de G. C., Las Palmas de Gran Canaria, Spain
[d] School of Engineering, Cardiff University, Cardiff, CF24 3AA, United Kingdom
[e] Scottish Power Energy Networks, Glasgow, G2 5AD, United Kingdom
[f] NTT Data UK, Birmingham, United Kingdom

ARTICLE INFO

Keywords:
Power distribution networks
Distributed energy resources
Dynamic power flow tracing
Loss allocation
P2P electricity market

ABSTRACT

This study explores peer-to-peer (P2P) electricity trading, emphasizing not just the export and consumption, but also the feasible physical supply of electricity and the use of distribution network assets. Building on a transaction-oriented dynamic power flow tracing model, a novel P2P market architecture is proposed. This architecture integrates the electricity market with the power network, considering technical constraints, network losses, and asset usage. The network is segmented into potential markets using second-order cone programming (SOCP), with an optimization problem introduced for loss-allocation. This problem merges network physical analysis and variable outputs from distributed energy resources (DERs). A graph-based P2P electricity trading model is designed to determine optimal transaction cost allocation and maximize benefits for both DERs and consumers. A case study on a modified IEEE 33-node test feeder substantiates the benefits of this market structure, demonstrating increased revenues for DERs and reduced bills for consumers compared to traditional feed-in-tariffs.

1. Introduction

The Climate Change Act to achieve a low-carbon economy was passed in the UK in 2008. Since then the reliance on fossil fuels and carbon emissions are continuously reduced by technological development, industrial transformation, and investment in renewable energy, without significantly sacrificing economic development [1]. Recent initiatives are launched to facilitate renewable distributed energy resources (DERs) including allowing local generation integration, investing in energy storage and accelerating the shift to zero-emission vehicles/electric vehicles [2]. From a market perspective, by introducing a range of new flexible strategies, DERs are encouraged to participate actively in newly forming market platforms, e.g. DNO Scottish & Southern Electricity Networks built two new platforms a "Neutral Market Facilitator" platform to register and track buyers and sellers of flexible electricity, and a "Whole System Coordinator" platform that will determine what its moment-to-moment grid needs are on 2020 [3]. At the same time, power network physical constraints cannot be overlooked so that overloading at peak times can be shaved, and network upgrade investments and operational costs can be minimized [4]. From 31 October to 12 November 2021, COP26, a critical summit for global climate action, in Glasgow marked a step forward in global efforts to limit warming to 1.5 degrees, global emissions by 2030 and achieve net-zero and carbon neutrality by 2050, where flexible markets which can encourage emission reduction will role significantly in this process in electricity industrial sector [5].

Traditionally, distribution network operators (DNOs) set connection char-ges for exporting and/or importing electricity. Even though now DER owners are allowed for grid connections and receiving incentives, their current interactions in the electricity market are only with the grid. In addition, the price is determined in advance (so-called feed-in tariffs (FiT)) by regulators [6] or suppliers [7]. For example, in the UK, the FiT of wind power is 2.88 p/kWh (pence per kilowatt-hour) when the capacity is between 100 and 1500 kW [8]. Conversely, a standard

☆ The work is supported by the Engineering and Physical Sciences Research Council (EPSRC, United Kingdom) in project "Street2Grid - an electricity blockchain platform for P2P energy trading" (Reference: EP/S001778/2).

* Corresponding author.
E-mail address: Jin.Yang@glasgow.ac.uk (J. Yang).

https://doi.org/10.1016/j.energy.2023.130120
Received 15 February 2023; Received in revised form 12 July 2023; Accepted 22 December 2023
Available online 27 December 2023

Nomenclature

Parameters

P_i^{load}	Active power of load at node i
Q_i^{load}	Reactive power of load at node i
U^{max}	Upper limit for voltage
U^{min}	Lower limit for voltage
R_{ij}	Branch resistance from node i to node j
X_{ij}	Branch reactance from node i to node j

Variables

P_i	Active power injection at node i
P_i^{DER}	Active power of DER at node i
P_{ij}	Branch active power vector from node i to node j
Q_i	Reactive power injection at node i
Q_i^{DER}	Reactive power of DER at node i
Q_{ij}	Branch reactive power vector from node i to node j
I_{ij}	Branch current vector from node i to node j
U_i	Voltage at node i
$I_{2,ij}$	Second-order decision variable of current from node i to node j
$U_{2,i}$	Second-order decision variable of voltage at node i
$\eta_i^{DER,share}$	The market share of DER at node i

Indices and sets

Ω_b	Set of all network branches

domestic electricity tariff is 17.493 p/kWh [9]. Recently, replacing FiT, the smart export guarantee (SEG) is launched as an obligation set by the UK government for licensed electricity suppliers to offer a tariff and pay for small-scale low-carbon generations of electricity exported to power grid companies, providing certain criteria are met, which came into force on 1st January 2020 [10]. However, even with the SEG, DER owners can only receive between 2 to 5.6 p/kWh which is decided by suppliers as long as it is not zero [11]. Therefore, under the existing market structure and regulations, market openness and fairness are far from ideal.

To further stimulate DER investments for local energy systems and general market participation, the economic profit margin between standard energy consumption tariff rates and export FiT/SEG should be released. Peer-to-peer (P2P) energy trading can directly link consumers with producers for mutual benefits, without intermediators such as suppliers [12]. However, P2P trading faces challenges that require radical changes, such as the existing centrally controlled grid, market architecture and regulations of current network connection charge models. Also, the P2P electricity prices should be reflected in an electricity retail market with competition openness.

The following sections explain model of P2P electricity market structure, summarize existing research and highlight the contributions of this paper, beyond the state-of-the-art.

1.1. Model explanation of P2P electricity market structure

Peer-to-peer (P2P) electricity markets can be organized in three main ways: community-based markets, fully decentralized markets, and 'composite' markets. Each type exhibits different structures and approaches to energy trading.

Community-based P2P market. This type of market is designed for customers and prosumers who are part of microgrids or neighborhoods. They typically have common interests and goals, and transactions are readily distributed by an aggregator. Various P2P trading models are established considering different aspects such as cheating behaviors, blockchain, and the uncertainty of photovoltaic (PV) generation. The analysis often involves optimization algorithms based on the alternating direction method of multipliers (ADMM).

Fully decentralized P2P market. In a fully decentralized P2P market, every participating prosumer can freely trade with others individually, with no centralized administration. All transactions between market participants rely on bilateral contracts. Every market participant aims to achieve its own optimal objective. A consensus and innovation algorithm is commonly used to link different participating individuals in the market and find the global optimum based on individual optimum.

'Composite' market. The 'composite' market is a combination of community-based and fully decentralized markets. Every single prosumer can freely trade with another within a community. Following intra-community trading, a community is represented by an aggregator or agent to trade with other communities. This approach ensures prosumers not only have fully open-trade options within their community but also are integrated as one actor, resulting in better bargaining power compared to individuals. Prosumers and communities join the market in parallel in a composite market. In this type of market, platforms have been implemented to test potential applications in real power systems.

1.2. Research challenge in P2P electricity market based on dynamic power flow tracing

According to previous model explanation, P2P electricity market structures are categorized into three types [23]: community-based markets [13–16], fully decentralized markets [17–19], and 'composite' markets [20–22]. A comparison of these types in terms of different participants' combinations is summarized in Table 1. Different studies have proposed and examined various P2P trading models [13–22]. While some focused on community-based markets [13–16], others proposed fully decentralized market models [17–19]. 'Composite' market structures [20–22] have also been explored, combining elements of the two previous types.

Existing research often overlooks non-traceable transactions that fail to reflect actual power transfers or asset usage within the physical network. Conventional loss allocation, typically necessitating an additional decomposition step [24], may overlook loss allocations, disproportionately assign them to all prosumers based on distributed energy resource outputs, or dismiss them as 'compensated by the main grid' or 'included in societal costs' [21]. This results in oversimplification of loss allocations and unjust grouping of participants without shared benefits.Power flow tracing techniques, which are useful in quantifying asset usage, recognize that not all generated power is utilized [25]. Power flow tracing techniques aims to manage losses while enforcing proportional sharing, deploying methodologies such as quadratic methods [26,27], direct loss coefficient [28], and circuit theory-based techniques [29,30]. However, within the horizon of power flow tracing – where only physics is the determinant – the primary goal of loss allocation is to handle losses during the application of proportional sharing. This accounts for the division of incoming flows among the nodal outflows in P2P trading.

In parallel, communities engaged in peer-to-peer (P2P) energy trading often face artificial segregation [13–15,21,22], which fails to take into account the dynamic nature of shared benefit groups. This dynamism arises from fluctuating power flows due to inconsistent renewable energy outputs and diverse demand profiles. From the perspective of a network operator, P2P energy transactions could be liable for usage-based fees within the distribution network [31]. Furthermore,

Table 1
Comparison of existing designs of three typical types of P2P market structure.

Paper	Participants	Innovation	Objective	Network losses	Algorithm
[13]	PV prosumers Energy storage owners	Consider dishonest players	Minimize social cost by energy cooperation	Only energy storage's loss	ADMM
[14,15]	Energy buildings	Create a building-centric framework/Mismatch of prediction values and actual values	Minimize the cost reduction ratio distribution/Minimize social energy cost; Clear for mutual energy sharing	Only energy storage's loss/Power network without congestion and losses	A dynamic best response based algorithm; ADMM
[16]	Prosumer microgrid	A penalty mechanism for changing energy sharing profiles	Maximize retails profit; Minimize prosumer expense	Transmission losses are neglected in local area	MILP problem
[17]	Individual prosumers	Captures both upstream downstream energy balance and forward market uncertainty	Utility-maximizing preferences for real time contracts and forward contracts	Losses are not explicitly considered, and need to be accounted for by a separate settlement process	Bilateral contracts
[18]	Microgrids with generators, inflexible flexible loads, and storage devices	Achieving global coordination to all the generators	The objective is to determine the settings of the components	No description	Consensus + innovations algorithm; ADMM
[19]	Agents of markets participants	Fully decentralized market with product differentiation	Distributed minimize each agent's expense	Losses are subject to social contracts	Relaxed Consensus + Innovation (RCI)
[20]	PV prosumers EV	Protect private information by blockchain	Minimize value-at-risk of energy sharing loss	The loss of energy distribution is neglected	A relaxation method-based algorithm/Blockchain
[21]	Community prosummers aggregator	Introduce community aggregators	Minimize the total social energy cost	Losses between communities are compensated by the main grid Losses in a community are neglected	A privacy-guaranteed ADMM
[22]	Nanogrid	A hybrid cyber–physical P2P energy sharing framework	Maximize the self-sufficiency; guarantee the stability of ES queues	No description	Lyapunov-based algorithm

network technical constraints can impact the feasibility of certain trades, suggesting a need to incorporate such factors in energy trading models [25]. Our proposed dynamic power flow tracing-based energy transaction model [11] advances technical research. For market design, a model incorporating this system is crucial. It guarantees precise energy loss allocation and a fair P2P energy market, dynamically adapting to renewable energy variability and demand, marking a significant stride in our continuous research.

The paper will present a novel approach to electricity market design and cost allocation, focusing on accurate power flow tracing and network segmentation for distributed energy resources. While not explicitly designed within the framework of the European Union's "Target Model" for electricity markets [32], our model resonates with the key principles of regional energy markets and market coupling. The precise allocation of energy and losses provides a more granular insight into market operations, especially in high DER penetration zones. Moreover, our model's segmentation facilitates local balancing of supply and demand while taking into account grid constraints, which mirrors the philosophy of market coupling. However, to completely align with the Target Model, there is a need for incorporating methods to enable cross-segment or cross-zone trade. Therefore, the proposed approach not only offers valuable improvements to existing energy market models but also sets the scene for future research aimed at developing a seamless market model spanning from local to regional levels.

1.3. Contributions

In this paper, a P2P market architecture based on dynamic power flow tracing is proposed. It boosts P2P engagements by a fair market based on transparent energy tracing and allocating transmission costs. The contributions of this study are summarized as follows:

- The potential of the P2P market with physical electricity system operation limits is explored — here we use the 'cocktail-layered energy market' as an analogy for market segmentation. Critical points of the different 'cocktail layers for market' segmentation are calculated by second-order cone programming. The proposed market segmentation principle fully considers the different scenarios of physically power flow. Loads which are powered by the same sources can be divided into the same community by the proposed principle.
- The loss function - a combination of an exponential function with a quadratic function, is designed for different types of DERs based on various market situations in individual market sharing models. With a fixed power factor, the percentage of DER's loss is in direct proportion with its output. Based on the approach proposed in this paper, the market price of a DER should be in inverse proportion to its output. Therefore, the output of a DER to achieve its maximum profit is pursued with a low loss proportion which is closely linked with the loss function in optimal power flows.
- The problem formulation is graph-based with nodes and links uniquely defined. Every participant is an optimization node in the graph connected by link constraints of different optimization functions. In this way, every participant's benefit is considered, while only price and power flow information is shared in the link constraints to ensure data privacy and security.
- A case study based on the IEEE 33-Node test feeder is conducted to verify the proposed power flow traceable P2P models. In a transparent open P2P market, (1) DER owners could maximize their revenue meanwhile have clear information of associated network losses (percentage share of their total output in an individual P2P transaction); (2) consumers could benefit from lower energy costs due to DERs' pricing strategies for being continuously competitive in this market; (3) the power supply quality from the grid can be potentially improved because the proposed market allows market dominance for DERs when they are located close to the tails of the network where voltage drops tend to be a problem.

The paper is organized as follows: Section 2 details the market segmentation and modeling. Section 3 presents the case study with two types of DERs (wind and PV) to prove benefit increase for every market participant. Section 4 summarizes the findings and concludes the paper.

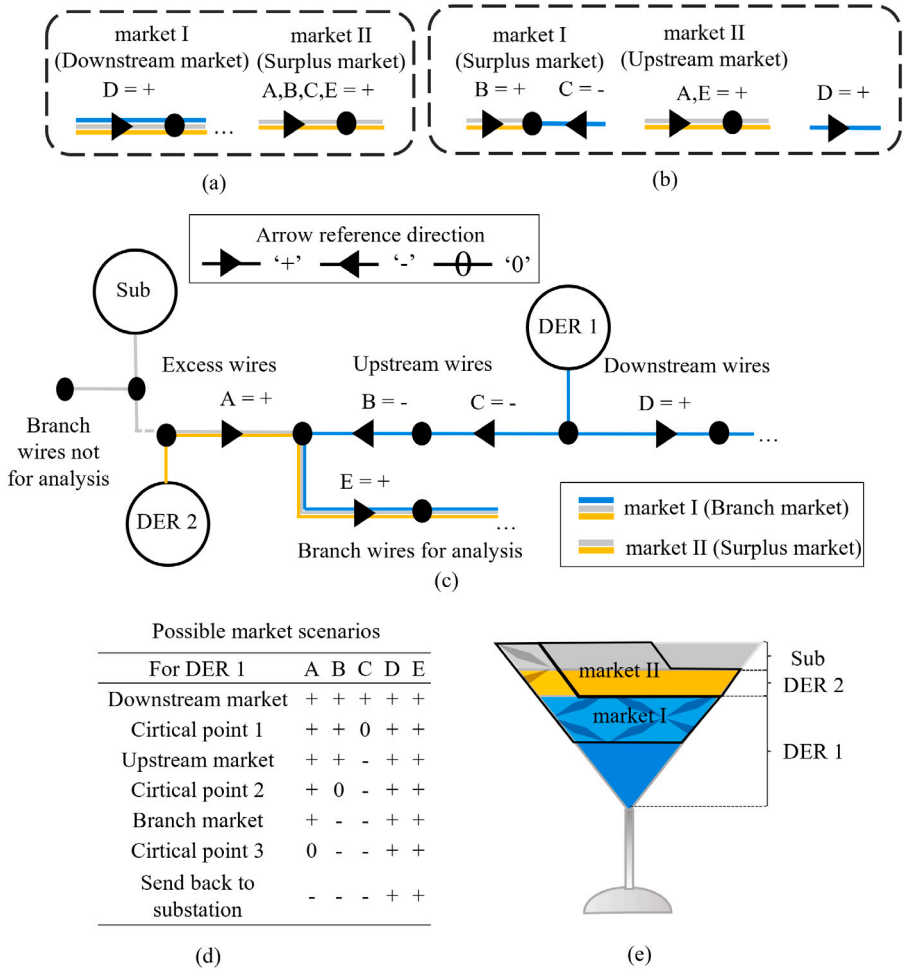

Fig. 1. Market segmentation based on dynamic power flow tracing.

2. Market segmentation and modeling

Addressing the challenge of quantifying power injection from specific generators that serve loads and incur losses across lines, power tracing becomes a crucial topic of research. Our previous study details the innovative approach of dynamic power flow tracing [11]. The focus of this paper is on the further application of this methodology, specifically exploring its implications for market segmentation. Here a novel model is proposed considering proportional sharing of energy and losses, which adds a unique dimension to this research. The model contributes to the growing body of knowledge in this area and demonstrates the novel and applied aspects of this study, thereby reinforcing the consistency and clarity of the research novelty.

2.1. Network segmentation

To integrate physical power flow tracing into the market segmentation, a power network is firstly segmented with the following definitions of wires and their references where applicable.

In a power network, different components play various roles. The longest path of the network, housing most of the buses, is termed as the 'backbone wires (cables)'. Connected to this backbone wire are 'branch wires for analysis', which significantly influence the flow tracing result. A crucial location within this configuration is the 'reference bus', positioned close to the tail end of the backbone wire. This is where a Distributed Energy Resource (DER) is typically located. The network further divides into 'downstream wires', linking the reference bus to the last bus on the tail, and 'upstream wires', connecting the reference bus to the first intersection of the backbone wire and branch counted from the reference bus. Finally, there are 'excess wires'. These constitute the remaining sections of the backbone wires, excluding the downstream and upstream wires. They also include other branches linked to the backbone wires but not designated for analysis. These branches are usually short, containing a small number of buses, and thus do not significantly impact the flow tracing result.

Considering a case with two DERs (generators) in one feeder from a substation (Sub) in top of Fig. 1. Backbone wires include wires between substation and the DER 2, wire A, wire B, wire C and wire D. The wire D connects to the end bus. The position of DER 1 is used as the reference bus to partition the network. B and C are upstream wires. D is the downstream wire. E is a branch wire for analysis. Wire A is an excess wire, including a branch not for analysis. For DER 1, once loads from DER1 downstream wires are fully fed by it, surplus power flows against the power flow from the substation. After loads on the wire E are fed by DER 1, electricity fed by DER 2 could be in reverse flows through the transformer. In addition, how DER 2 can feed to the network depends on power from DER 1.

2.2. Market segmentation principle

Under this assumption, DERs located close to the tails of the network have the market dominance — as naturally power flows will follow low impedance routes. This leads to the fact that the market segmentation fully depends on power flow tracing results. For example, DER 1 and DER 2 shown in Fig. 1 both have the ability to cover all loads' needs in the network. As DER 1 is located in the tail of the

system, DER 1 will take all loads (e.g.loads from downstream wires, upstream wires and branch wires for analysis shown in Fig. 1) and DER 2 only can sell its power to upper-level substations.This in fact can encourage DERs to be installed within and towards the tails of the network where potential voltage drop issues can be alleviated. Conversely, with high DER penetration, voltage increase can be solved by cutting output. DG maximum output which is automatically set by the upper limit of voltage upper limit in following Section 2.2 Market Segmentation Model, Eq. (2). The active power market-entry limitation of one generator is obtained by setting the corresponding wire active power as 0. Base on the above, 'branch market' is defined as customers being fed by the substation or DERs connected to other branches, when the local DER cannot meet load demand or there is no DER available locally in the branch wire for analysis. For example, by setting the active power of wire B as 0, the active power of DER 1 is its market-entry limitation for the 'branch market'. If DER 1 wants to get in the 'branch market', its active power output should be larger than the above limit. These active power market-entry limitations are named as 'critical points' between different markets.

Arrow directions of A, B, C, D and E are active power flow directions. '+' corresponds to flows in the same direction as that radial coming from the substation and '−' corresponds to flows in the opposite direction. '0' means there is no active power flow in this wire. The 'branch market' situation is shown in Fig. 1 as an example, where arrow directions of A, D, E are '+'. Arrow directions of B and C are '−'. Loads from downstream and upstream wires are fully supplied by DER 1. The flows through wires B (from DER 1) and A (from DER 2 and the substation) converge to wire E. Therefore, the branch market is open for P2P competitions. Possible market scenarios are listed in the table of Fig. 1(d).

The markets under consideration can be categorized into two main types, namely Market I and Market II. Market I is comprised of three submarkets: the downstream market, the upstream market, and the branch market. The downstream market operates in the downstream wires, where the arrow directions of nodes A, B, C, D, and E are all positive, indicating that loads are supplied by DER 1, DER 2, and the substation. In contrast, the upstream market operates in the upstream wires. Here, the arrow directions of nodes A, B, D, and E remain positive, but node C's direction is negative. The implication is that the loads in the upstream market are supplied by DER 1, DER 2, and the substation, with loads from DER 1 downstream wires being exclusively supplied by DER 1. The branch market is a separate entity that operates under conditions previously described.

Market II, on the other hand, is characterized by a surplus market. This is the market that comes into play after Market I has been accounted for. The loads in the surplus market are supplied by DER 2 and the substation. This market is designed to optimize the allocation of surplus energy produced by DER 2 and the substation. These market classifications offer a robust framework for optimizing the utilization of energy resources, ensuring that demand is met efficiently across different segments of the network.

Only one area of loads from downstream, upstream and branch can be fed by all of DER 1, DER 2 and the substation. Therefore, only one market of the downstream market, upstream market and branch market can exist at one time, marked as 'market I'. The surplus market happens with one of the above three markets at the same time, marked as 'market II'. In this case, network loads are met ('filled') by DER 1, DER 2 and the substation in order.

2.3. Market segmentation model

These newly defined critical points in Section 2.1 can be identified with the minimum absolute value of specified branch active power by means of second-order cone programming (SOCP) [33]. DERs' outputs are controllable variables. Critical point 1 means that DER 1 output well matches loads from DER1 downstream wires. Critical point 2 means that DER 1 output can fulfill loads from DER1 downstream wires plus loads from DER 1 upstream wires. Critical point 3 means that DER 1 output plus DER 2 output equal to loads from DER1 downstream wires plus loads from DER 1 upstream wires plus loads from the branch for analysis. DER outputs for different critical points, $P_i^{DER,cp}$, can be calculated when the value of specified branch active power is close to 0, e.g. the branch are A, B or C near the bifurcation branch E or DER 1, as shown in Fig. 1. An analogy of the market segmentation based on power flow tracing is 'a layered cocktail' that has a sequentially filled characteristic, where critical points are similar to the liquid interfaces between different layers in a cocktail, as shown in Fig. 1(e).

$$min\,|P_{ij}|\ ;\forall ij = A,\ B\ or\ C \tag{1}$$

Power flow constraints:

$$\begin{cases} \sum_{ik\in\Omega_b} P_{ik} = \sum_{ij\in\Omega_b} (P_{ji} - R_{ji}(I_{ji})^2) + P_i \\ \sum_{ik\in\Omega_b} Q_{ik} = \sum_{ij\in\Omega_b} (Q_{ji} - X_{ji}(I_{ji})^2) + Q_i \\ P_i = P_i^{DER} - P_i^{load} \\ Q_i = Q_i^{DER} - Q_i^{load} \\ (U_i)^2 = (U_j)^2 - 2(R_{ji}P_{ji} + X_{ji}Q_{ji}) + (R_{ji}^2 + X_{ji}^2)(I_{ji})^2 \\ U^{min} \le U_i \le U^{max} \end{cases} \tag{2}$$

By replacing $(I_{ij})^2$ and $(U_i)^2$ with $I_{2,ij}$ and $U_{2,i}$, the model of network in the second-order cone programming is formulated as follows:

$$\begin{cases} \sum_{ik\in\Omega_b} P_{ik} = \sum_{ij\in\Omega_b} (P_{ji} - R_{ji}(I_{2,ji})) + P_i \\ \sum_{ik\in\Omega_b} Q_{ik} = \sum_{ij\in\Omega_b} (Q_{ji} - X_{ji}(I_{2,ji})) + Q_i \\ P_i = P_i^{DER} - P_i^{load} \\ Q_i = Q_i^{DER} - Q_i^{load} \\ (U_{2,i}) = (U_{2,j}) - 2(R_{ji}P_{ji} + X_{ji}Q_{ji}) + (R_{ji}^2 + X_{ji}^2)(I_{2,ji}) \\ (U^{min})^2 \le U_{2,i} \le (U^{max})^2 \end{cases} \tag{3}$$

$$I_{2,ij} = \frac{(P_{ij}^2 + Q_{ij}^2)}{U_{2,ij}} \quad i,j \in B \tag{4}$$

Eq. (4) can be further loosened and transformed into the form of SOCP.

$$\|[2P_{ij} \quad 2Q_{ij} \quad I_{2,ij} - U_{2,ij}]^T\|_2 \le I_{2,ij} + U_{2,ij} \tag{5}$$

The generation share that a DER can participate within a market is calculated by the following equation:

$$\eta_i^{DER,share} = \frac{P_i^{DER} - P_i^{DER,cp}}{P_i^{DER}} \tag{6}$$

where $\eta_i^{DER,share}$ is the market share of DER at node i.

2.4. Individual market loss allocation model

The loss function is defined as the combination of an exponential function and a quadratic function. This definition enables limiting the error within the range of 10^{-3} [34]:

$$f^{loss}(x) = m \cdot ln(x) + ax^2 + bx + c \tag{7}$$

where f^{loss} represents $(1 - P_i^{DER_{loss}}/P_i^{DER})$, loads percentage of DER active power output (excluding losses) at node i; $P_i^{DER_{loss}}/P_i^{DER}$ represents network loss percentage of one DER active power output ; x represents $P_i^{DER}/\sum P^{load}$, one DER active power percentage of whole

network loads. Therefore, $P_i^{DER_{noloss}}$ is active power output from DER except for its accounts for the losses

$$P_i^{DER_{noloss}} = f^{loss}\left(\frac{P_i^{DER}}{\sum P^{load}}\right) \cdot P_i^{DER} \tag{8}$$

When one DER active power percentage ($P^{DER}/\sum P^{load}$) increases, the load area transferred by this DER increases. Therefore, an DER accounts for more losses in the network as its power is transferred to the loads further than before ($P_i^{DER_{loss}}/P_i^{DER}$ increases and f^{loss} decreases).

2.5. Individual DER cost and income model

The cost function is designed as follows:

$$Cost_i^{DER} = Cost^{Grid} - \alpha Cost^{Grid} \cdot \frac{P_i^{DER}}{P_i^{DER,max}} \quad 0 < \alpha \le 0.5 \tag{9}$$

$$-\alpha \cdot \frac{Cost^{Grid}}{P_i^{DER,max}} < 0 \tag{10}$$

$$Cost^{Grid} - 2\alpha \cdot \frac{Cost^{Grid} \cdot P_i^{DER}}{P_i^{DER,max}} \ge 0 \tag{11}$$

where the DER income function is $Income^{DER} = Cost^{DER} \cdot P^{DER}$, $P_i^{DER,max}$ is the maximum active power of DER at node i. By setting the cost factor α meeting, the derivative of cost function is less than zero, as expressed in Eq. (10) and the income function is not negative, as expressed in Eq. (11). It satisfies that the total income increases when DERs increase outputs until their maximum capacities, even though marginal cost decreases. This motivates DER to increase their DER outputs whilst decreasing customer electricity purchase cost.

2.6. Model implementation

The models described in the previous section within the P2P energy market are implemented with OptiGraph (a general graph-based modeling abstraction for optimization), built with a set of OptiNodes (each embedding an optimization model with its local variables, constraints, objective function and data) and a set of OptiEdges (each embedding a set of linking constraints) [35]. The OptiGraph as an undirected hypergraph contains the optimization model of interest. The OptiEdges are hyperedges that connect two or more OptiNodes. Modeling details are further presented in Appendix.

2.6.1. OptiNode model for $load_a$

Here a represents a set of loads in market I and market II. The $load_a$'s objective is to minimize its electricity purchase cost.

$$\begin{aligned} \min \quad & Cost_i^{DER} \cdot P_i^{DER-load_a} + Cost^{Grid} \cdot P^{Grid-load_a} \\ \text{s.t.} \quad & P_i^{DER-load_a} + P^{Gird-load_a} = P_i^{load_a} \\ & P_i^{DER-load_a}, P^{Gird-load_a} \ge 0 \end{aligned} \tag{12}$$

where $Cost^{Grid}$ is the electricity cost from the substation; $P_i^{DER-load_a}$ is the active power from DER at node i to $load_a$; $P_i^{Gird-load_a}$ is the active power from substation to $load_a$.

2.6.2. OptiNode model for DER

Each DER's objective is to maximize its total income.

$$\begin{aligned} \max \quad & Cost^{DER}i \cdot P_i^{DERnoloss} \\ \text{s.t.} \quad & Cost_i^{DER} \le Cost^{Grid} \\ & P_i^{DER} \le P_i^{DER,max} \\ & Cost_i^{DER} = Cost^{Grid} - \alpha Cost^{Grid} \cdot \frac{P_i^{DER}}{P_i^{DER,max}} \\ & 0 < \alpha_i \le 0.5, and, (8) \end{aligned} \tag{13}$$

2.6.3. OptiEdges for linking constraints

Linking constraints include cost linking constraints and power linking constraints.

Cost linking equations: The cost provided by DERs equals to the cost received by customers.

Power linking equations: DER outputs in markets equals to all loads in markets.

$$P_i^{DER_{noloss}} \cdot \eta_i^{DER,share} = \sum P_i^{DER-load_a} \tag{14}$$

3. Case study

The proposed P2P model and market segmentation algorithms are implemented and validated in this section. The detailed procedure of implementing the proposed P2P market model and algorithms is shown in Fig. 2, based on Python and Julia [36].

The segmentation of the market is a vital step in the overall process. Critical points for different markets are accurately calculated using second-order cone programming (SOCP), implemented via the JuMP package in Julia [37]. Once the markets are defined, the subsequent focus shifts to defining Market I and Market II. This process leverages the power flow tracing model, as described in earlier work [11]. The power flow calculations are facilitated by the Pandapower Python package [38], which provides reliable and efficient power flow results. With the markets defined and the power flow calculated, attention turns to determining the loss functions. These are modeled using the Python package, scipy.optimize.curve_fit [39], known for its robust curve fitting abilities. The error tolerance is set at 10^{-3}, ensuring accurate and reliable results. Finally, peer-to-peer energy market trading is addressed, relying on a model based on graph theory. The implementation of this complex model is realized using the Plasmo Julia package [35]. This systematic approach ensures an efficient and fair peer-to-peer energy market, enhancing the benefits for both distributed energy resources and consumers.

The computing environment used to simulate the proposed model is Intel i7-10850H 2.7 GHz CPU, 32 GBRAM, Linux (Ubuntu). The IEEE 33-node test feeder, a 12.66 kV radial distribution system is used for this case study. The original circuit is modified by installing two DERs: a 2 MVA wind power turbine (DER 1) at bus 14 and a 3 MVA solar photo-voltaic (PV) plant (DER 2) at bus 20. The power factor of DER 1 and DER 2 are 0.62. The topology of the circuit is shown in Fig. 3(a). The profiles of DER 1, DER 2 and all the loads are shown in Fig. 3(b).

3.1. Market segmentation result

The backbone wires of the IEEE 33-node test feeder are from buses 1 to 18 which is the longest path of the network with 18 buses. The bus 14 where the DER 1 locates is the reference bus. Considering all DERs are under maximum output condition, four load areas are categorized as follows: DER 1 downstream wires (from buses 15 to 18), DER 1 upstream wires(from buses 7 to 13), bus 6 with its branch (bus 6 and branch wires for analysis from buses 26 to 33), DER 2 branch wires (from buses 19 to 22), and the excess wires (the rest backbone wires from buses 1 to 6, and branch wires not for analysis from buses 23 to 24), as shown in Fig. 3(a) and Table 2. Colors are used to visualize different markets in 24 h.

Table 2 shows the potential for flexible utilization of surplus generation, where DERs have the freedom to sell a portion of their excess power in P2P transactions, guided by power flow tracing results. This implies that DERs can participate in bilateral transactions with other market participants, conforming to a transaction-oriented dynamic power flow tracing model. Thus, both customers and DERs can establish bilateral contracts, in alignment with the quantification of power contributions from specific generators that service loads and induce losses across transmission lines. Furthermore, this form of cost allocation is primarily utilized in an ex ante fashion, serving as a

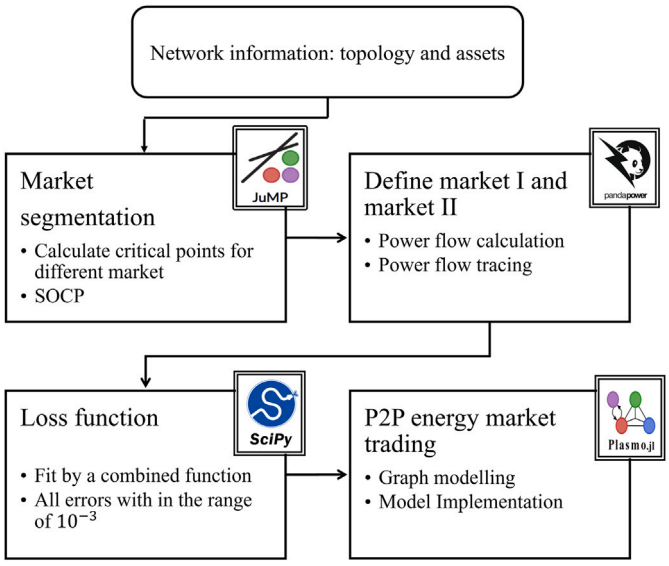

Fig. 2. Flow chart of the implementation process with the proposed P2P market model, functions and algorithms.

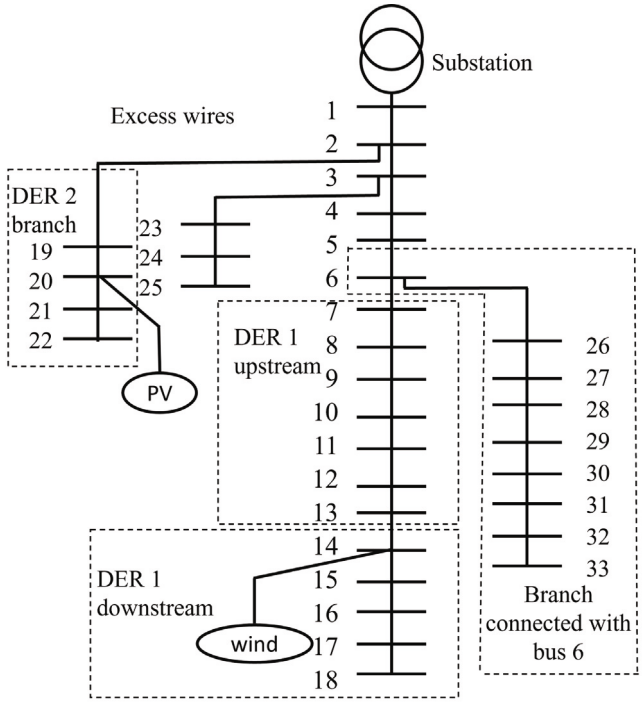

(a) Topology of the IEEE 33-node test network

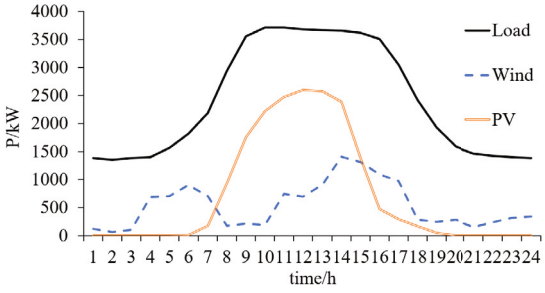

(b) PV, wind generation and total load profiles

Fig. 3. Test network with IEEE 33-node test network topology and profiles.

predictive tool. However, its potential extends to ex post applications as well, where it could be employed for retrospective analysis and adjustment of transactions, thereby ensuring a more accurate and fair allocation of costs based on actual power flows and usage. This dual utility enhances the robustness and flexibility of our energy market design framework, enabling it to adapt to the dynamic nature of power generation and consumption.

DER 1 downstream market (including DER 1 downstream wires): From hours 1 to 3, loads are supplied by both substation and DER 1. From hours 8 to 10, loads are supplied by the substation, DER 1 and DER 2.

DER 1 upstream market (including DER 1 upstream wires): From hours 11 to 13, loads are supplied by substation, DER 1 and DER 2. From hours 18 to 24, loads are supplied by substation and DER 1.

Branch market connected with bus 6 (including bus 6 with its branch wires): From hours 4 to 7, loads are supplied by both the substation and DER 1. From hours 14 to 17, loads are supplied by the substation, DER 1, and DER 2.

Surplus market: In hours 6, 7, 18, and 19, there are sporadic markets between DER 2 and substation. These markets are independent of the markets between DER 1 and substation. Therefore, these markets can be ignored considering DER 2 output is small. However, between hour 8 and hour 17, the surplus market at least includes all loads from excess buses and can influence market I. Therefore, the surplus market is considered during this period.

3.2. Individual market sharing result

Active power market-entry limitations of DERs are shown in Table 3. By setting $P_{ij}{}_{\substack{i=13\\j=14}}$, $P_{ij}{}_{\substack{i=6\\j=7}}$, $P_{ij}{}_{\substack{i=5\\j=6}}$ as 0, active power market-entry upper limitations of the downstream generator can be obtained as 10.52%, 30.04% and 58.44%. 3.23% means DER 1 located in bus 14 can meet the demand of the local load. Based on the DER 1 market $P_{ij} = 0$ condition, by setting $P_{ij}{}_{\substack{i=1\\j=2}}$ as 0, upper limitations of the downstream generator for different markets can be obtained as 110.23%, 96.99% and 74.95%. 10.24% means DER 2 located in bus 20 can meet the demand of loads from the branch (bus 19 to bus 22). Different loss functions for different DERs in different market situations are shown in Fig. 4. Fitted loss functions' parameters are shown in Table 4. All parameters are defined in Eq. (7) and they are sampling and calculated by the Python package scipy.opt-imize.curve_fit [39].

For the DER 1 power generator, in the test system, the loss function curve can be divided into three parts: constant (zero deceleration), increasing deceleration, constant deceleration, corresponding to three market situations: DER 1 downstream, DER 1 upstream, and Branch market. For DER 2 in the test system, when it can get into more markets, it shares more losses even with the same output because it can transfer power to loads farther away. Therefore, the slope of the loss function of DER 2 can be sorted from the largest to the smallest as: DER 1 downstream > DER 1 upstream > Branch market connected with bus 6.

3.3. Market costing results

3.3.1. Individual costs and DER outputs

The cost function is shown in Fig. 5, with an assumption that $\alpha^{DER1} = \alpha^{DER2} = 0.5$. When DER 1 reaches its maximum output of 1405.14 kW or DER 2 reaches its maximum output of 2600.50 kW, they can provide energy at a its electricity purchase cost of 8.747 p/kWh (pence per kilowatt-hour), half of the standard electricity tariff of 17.493 p/kWh [40] (accessed Jul. 15, 2020). However, the its electricity purchase cost of energy provided by DERs, at 8.747 p/kWh, is higher than the feed-in tariff (2.28 p/kWh for DER 1 and 0.33 p/kWh for DER 2 [8]). As the output from the DERs increases, the unit cost of energy from DERs decreases, but their total income increases.

Table 2
24-h power flow tracing results for the IEEE 33-node test network.

time/h

		1	2	3	4	5	6	7	8	9	10	11	12	13	14	15	16	17	18	19	20	21	22	23	24
Excess wires	1	100	100	100	100	100	100	100	100	100	100	100	100	100	100	100	100	100	100	100	100	100	100	100	100
	2	100	100	100	100	100	100	100	110	110	110	110	110	110	110	110	110	110	100	100	100	100	100	100	100
	3	100	100	100	100	100	100	100	110	110	110	110	110	110	110	110	110	110	100	100	100	100	100	100	100
	4	100	100	100	100	100	100	100	110	110	110	110	110	110	110	110	110	110	100	100	100	100	100	100	100
	5	100	100	100	100	100	100	100	110	110	110	110	110	110	110	110	110	110	100	100	100	100	100	100	100
	6	100	100	100	101	101	101	101	110	110	110	110	110	110	111	111	111	111	100	100	100	100	100	100	100
DER 1 upstream	7	100	100	100	001	001	001	001	110	110	110	110	110	111	001	001	001	001	100	100	100	100	100	100	101
	8	100	100	100	001	001	001	001	110	110	110	111	111	001	001	001	001	001	100	100	100	100	100	101	001
	9	100	100	100	001	001	001	001	110	110	110	001	001	001	001	001	001	001	100	100	101	100	101	001	001
	10	100	100	100	001	001	001	001	110	110	110	001	001	001	001	001	001	001	100	100	001	100	001	001	001
	11	100	100	100	001	001	001	001	110	110	110	001	001	001	001	001	001	001	100	100	001	100	001	001	001
	12	100	100	100	001	001	001	001	110	110	110	001	001	001	001	001	001	001	100	101	001	100	001	001	001
	13	100	100	100	001	001	001	001	110	110	110	001	001	001	001	001	001	001	101	001	001	101	001	001	001
DER 1 downstream	14	001	001	001	001	001	001	001	001	001	001	001	001	001	001	001	001	001	001	001	001	001	001	001	001
	15	101	101	101	001	001	001	001	111	111	111	001	001	001	001	001	001	001	001	001	001	001	001	001	001
	16	101	101	101	001	001	001	001	111	111	111	001	001	001	001	001	001	001	001	001	001	001	001	001	001
	17	101	101	101	001	001	001	001	111	111	111	001	001	001	001	001	001	001	001	001	001	001	001	001	001
	18	101	101	101	001	001	001	001	111	111	111	001	001	001	001	001	001	001	001	001	001	001	001	001	001
DER 2 branch	19	100	100	100	100	100	100	100	110	010	010	010	010	010	010	010	010	010	010	100	100	100	100	100	100
	20	100	100	100	100	100	100	110	010	010	010	010	010	010	010	010	010	010	010	010	010	100	100	100	100
	21	100	100	100	100	100	100	100	010	010	010	010	010	010	010	010	010	010	010	110	110	100	100	100	100
	22	100	100	100	100	100	100	100	010	010	010	010	010	010	010	010	010	010	010	110	110	100	100	100	100
Excess wires	23	100	100	100	100	100	100	100	110	110	110	110	110	110	110	110	110	110	110	100	100	100	100	100	100
	24	100	100	100	100	100	100	100	110	110	110	110	110	110	110	110	110	110	110	100	100	100	100	100	100
	25	100	100	100	100	100	100	100	110	110	110	110	110	110	110	110	110	110	110	100	100	100	100	100	100
Branch connected with bus 6	26	100	100	100	101	101	101	101	110	110	110	110	110	110	111	111	111	111	100	100	100	100	100	100	100
	27	100	100	100	101	101	101	101	110	110	110	110	110	110	111	111	111	111	100	100	100	100	100	100	100
	28	100	100	100	101	101	101	101	110	110	110	110	110	110	111	111	111	111	100	100	100	100	100	100	100
	29	100	100	100	101	101	101	101	110	110	110	110	110	110	111	111	111	111	100	100	100	100	100	100	100
	30	100	100	100	101	101	101	101	110	110	110	110	110	110	111	111	111	111	100	100	100	100	100	100	100
	31	100	100	100	101	101	101	101	110	110	110	110	110	110	111	111	111	111	100	100	100	100	100	100	100
	32	100	100	100	101	101	101	101	110	110	110	110	110	110	111	111	111	111	100	100	100	100	100	100	100
	33	100	100	100	101	101	101	101	110	110	110	110	110	110	111	111	111	111	100	100	100	100	100	100	100

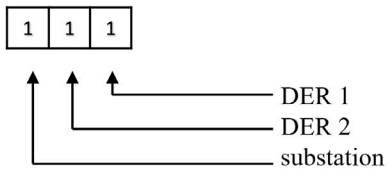

If the bus is supplied by the source, the corresponding digit is noted as 1 otherwise 0. E.g., 111 means this bus is supplied by DER 1, DER 2 and substation.
111 or 101 represents market I
110 represents market II.

Table 3
Active power market-entry limitations of DERs.

	DER 1 downstream	DER 1 upstream	Branch market connected with bus 6
Market bus	15 to 18	7 to 13	26 to 33 and 6
$P_{ij}=0$ (DER 1 market)	i = 13, j = 14	i = 6, j = 7	i = 5, j = 6
$\frac{P_{DER1}}{\sum P_{load}}$	3.23% ~ 10.52%	10.52% ~ 30.04%	30.04% ~ 58.44%
Power factor (DER 1)	0.85	0.85	0.97
Voltage at DER 1	0.95	1	1.04
$P_{ij}=0$ (DER 2 market)	i = 1, j = 2	i = 1, j = 2	i = 1, j = 2
$\frac{P_{DER2}}{\sum P_{load}}$	10.24% ~ 110.23%	10.24% ~ 96.99%	10.24% ~ 74.95%
Power factor (DER 2)	0.84	0.85	1
Voltage at DER 2	1.07	1.05	1.03

The cost allocation for different consumers and the resulting outputs from the DERs are detailed in Table 5. Market I is one of the three markets (downstream of DER 1, upstream of DER 1, and the Branch market connected with bus 6). It comprises buses supplied by DER 1 and the substation constantly, and includes buses supplied by DER 2 between the 8th and 17th hours. Market II is the surplus market, comprising only buses supplied by DER 2 and the substation, excluding DER 1, between the 8th and 17th hours. The cost for loads in a market can be calculated as $\sum(P^{DER} * Cost^{DER} + P^{Sub} * Cost^{Sub})/P^{load}$. For other loads not included in a market, their tariffs are determined by their respective electricity sources.

As a DER increases its output, its per unit cost decreases, but the losses it must share increase. From the 1st to 7th hour and 18th to 24th hour, the cost in Market I is higher than the cost from DER 1 and lower than 17.493 p/kWh. The average output portions in Market I from the 8th to 10th hours are $P^{DER1} : P^{DER2} : P^{Sub} = 33\% : 32\% : 34\%$, and from the 11th to 13th hours $P^{DER1} : P^{DER2} : P^{Sub} = 58\% : 32\% : 10\%$. From the 8th to 13th hours, the Market I cost lies between the costs from DER 1 and DER 2.

Meanwhile, the cost in Market I is lower than in Market II. The average output portion in Market I from the 14th to 18th hours is $P^{DER1} : P^{DER2} : P^{Sub} = 14\% : 33\% : 53\%$. From the 14th to 18th hours, DER 1's exclusive market is larger than in the previous two time periods, hence there is insufficient DER 1 power to supply the branch market connected with bus 6 (below 15%). From the 8th to 17th hours, the cost in Market II is higher than the cost from DER 2 and lower than 17.493 p/kWh.

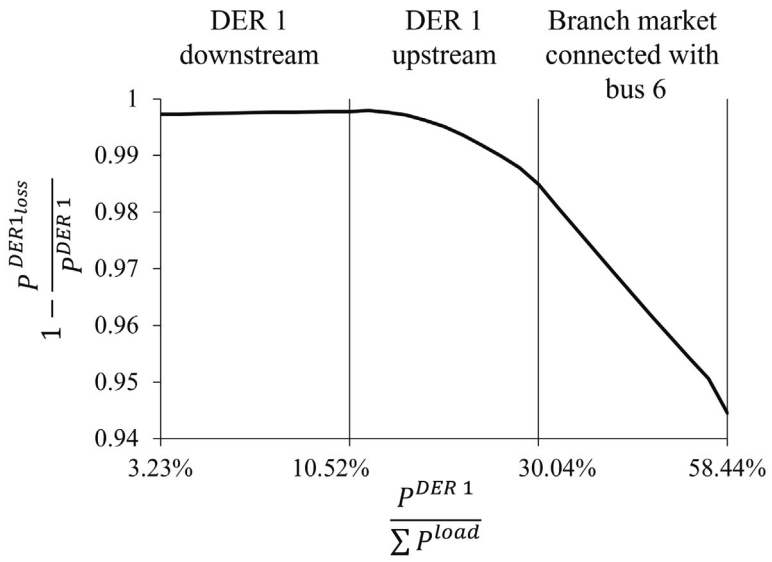

(a) Loss percentage $(1-\frac{P^{DER1_{loss}}}{P^{DER1}})$ and DER percentage $(\frac{P^{DER1}}{\sum P^{load}})$ functions of DER 1

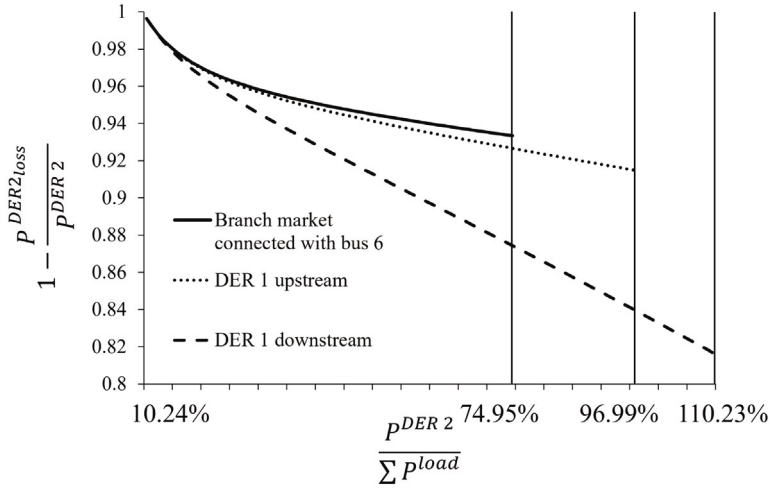

(b) Loss percentage $(1-\frac{P^{DER2_{loss}}}{P^{DER2}})$ and DER percentage $(\frac{P^{DER2}}{\sum P^{load}})$ functions of DER 2

Fig. 4. Loss functions of DERs in different markets.

Table 4
Loss function parameters.

	Loss index of DER 1			Loss index of DER 2		
	DER 1 downstream market	DER 1 upstream market	Branch market connected with bus 6	DER 1 downstream market	DER 1 upstream market	Branch market connected with bus 6
m	0	0	0	−0.0361	−0.0464	−0.0356
a	0	−0.4370	0	−0.0510	−0.0492	0
b	0	0.0937	−0.1376	−0.0312	0.0800	0.0019
c	0.9975	0.9927	1.0220	0.9162	0.8813	0.9100
Error[a]	1.63E−04	2.71E−04	6.04E−04	3.92E−04	4.10E−04	8.67E−04

[a] Standard error of the regression.

3.3.2. Customer total energy costs

Collectively, consumers can save £1736.44, $\sum(P^{DER} - P^{DER_{loss}} \times (Cost^{Sub} - Cost^{DER}))$ for a span of 24 h, as shown in Eq. (15) and outlined in Table 5. DER 1 and DER 2 can increase their revenue by £1264.58 and £1910.79 respectively, $\sum P^{DER} \times (Cost^{DER} - Cost^{feed-in\,tariff})$. The calculation process is analogous to the savings calculation for consumers, and is omitted here to avoid repetition. Details about the savings made by consumers and increased revenues of the DERs are shown in Table 6. Broadly, when consumers consume more energy from the DERs, they save more money, both in aggregate and per unit. Conversely, when DERs generate more energy, their total

Table 5
P2P electricity purchase cost and DER output results.

Time h	DER 1 cost p/kWh	DER 1 output kWh	DER 1 loss kWh	DER 2 cost p/kWh	DER 2 output kWh	DER 2 loss kWh	Market I p/kWh	Market II p/kWh
1	16.75	119.18	0.30	–	–	–	16.95	–
2	17.07	68.00	0.17	–	–	–	17.39	–
3	16.84	104.95	0.26	–	–	–	17.10	–
4	13.22	686.99	30.90	–	–	–	14.61	–
5	13.12	702.45	27.58	–	–	–	15.20	–
6	11.90	899.17	40.95	–	–	–	13.63	–
7	13.09	706.97	15.62	–	–	–	17.22	–
8	16.42	172.05	0.43	14.35	934.92	53.74	16.17	16.68
9	16.16	214.79	0.53	11.60	1752.47	150.78	15.16	14.87
10	16.33	187.57	0.47	10.02	2221.91	227.05	14.38	13.40
11	12.87	742.79	4.48	9.18	2471.29	342.66	10.77	11.05
12	13.16	696.32	3.62	8.75	2600.50	324.45	10.06	10.02
13	11.81	913.32	10.13	8.86	2566.33	307.03	9.74	8.86
14	8.75	1405.14	42.73	9.48	2383.84	181.07	9.52	9.60
15	9.30	1315.47	36.33	12.84	1382.91	78.09	13.96	15.09
16	10.70	1091.33	22.24	15.90	473.95	8.99	17.21	17.35
17	11.45	970.41	20.80	16.49	297.91	2.21	17.19	17.46
18	15.69	289.05	0.68	–	–	–	17.41	–
19	15.95	248.55	0.62	–	–	–	17.37	–
20	15.71	285.82	1.31	–	–	–	17.05	–
21	16.53	154.55	0.35	–	–	–	17.49	–
22	16.02	236.12	0.89	–	–	–	17.20	–
23	15.50	320.60	2.79	–	–	–	16.69	–
24	15.38	338.73	3.56	–	–	–	16.53	–

p/kWh - British pence per kilowatt-hour.

Table 6
Consumers' cost reductions and DERs' income increases.

Time/h	Average £ per hour							p per kWh						
	1 to 3	4 to 7	8 to 10	11 to 13	14 to 17	18 to 24	24 h	1 to 3	4 to 7	8 to 10	11 to 13	14 to 17	18 to 24	24 h
DER 1 downstream	0.62	8.90	5.75	18.88	28.32	1.35	9.70	0.64	4.68	2.33	4.88	7.51	1.66	3.43
DER 1 upstream	0.00	15.64	14.74	38.48	49.74	2.88	18.27	0.00	4.68	2.63	5.66	7.51	1.66	3.48
Branch connected with bus 6	0.00	9.46	21.09	52.28	28.94	0.00	15.57	0.00	2.19	2.63	8.02	3.17	0.00	2.22
Excess buses	0.00	0.00	35.73	88.56	33.41	0.00	21.10	0.00	0.00	2.63	8.02	2.76	0.00	1.79
DER 2 branch	0.00	0.00	14.06	30.60	9.98	0.00	7.25	0.00	0.00	5.68	8.56	3.96	0.00	2.44
Sum	0.62	34.01	91.38	228.81	150.39	4.23	71.89	0.64	11.55	15.91	35.13	24.91	3.32	13.37
DER 1 increased income	14.15	74.89	26.75	79.72	88.07	34.49	50.86	14.54	10.00	13.97	10.17	7.37	13.48	11.10
DER 2 increased income	0.00	0.00	165.30	189.84	121.00	0.00	64.56	0.00	0.00	10.10	7.46	10.66	0.00	3.97
Sum	14.15	74.89	192.05	269.55	209.07	34.49	115.42	14.54	10.00	24.07	17.63	18.03	13.48	15.07

revenue increases, but their per-unit revenue decreases.

$$\begin{aligned}&\sum_{t}^{24\,\mathrm{h}}(P^{DER}-P^{DER_{loss}})\times(Cost^{Sub}-Cost^{DER})\\&=(119.18\ \mathrm{kWh}-0.30\ \mathrm{kWh})\times(17.49\ \mathrm{p/kWh}-16.75\ \mathrm{p/kWh})+\cdots\\&\quad+(338.73\ \mathrm{kWh}-3.56\ \mathrm{kWh})\times(17.49\ \mathrm{p/kWh}-15.38\ \mathrm{p/kWh})\\&=1736.44\end{aligned}\tag{15}$$

Time analysis for the market: From hours 11 to 13, for customers from the branch connected with bus 6, excess buses and DER 2 branch, they can save the most money (52.28, 88.56 and 30.60 average £ per hour & 8.02, 8.02 and 8.56 p/kWh) both in total and per unit. This is because the combined output from the DERs is highest during this period. But from hours 14 to 17, for customers from DER 1 downstream and DER 1 upstream, they can save the most (28.32 and 49.74 average £ per hour & 7.51 and 7.51 p/kWh) both in total and per unit. This is because the total output from DER 1 is highest during this period, and customers from DER 1 downstream and DER 1 upstream are predominantly supplied by DER 1.

Spatial analysis for the market: Customers from the excess buses can save the largest sum of money (21.10 £ per hour) over 24 h because their total demand is highest. Customers from DER 1 upstream can save the most money per unit (3.48 p/kWh) over 24 h. This is primarily because they are supplied with energy from DERs most of the time, and from hours 11 to 13, they can get a better cost rate than customers from DER 1 upstream, as part of their energy is supplied by DER 2.

These results and analyses demonstrate that a P2P market based on power flow tracing can unlock potential economic values within local energy systems. Network losses can be distinctly traced to DERs, and market segmentation links the trading with the usage of the physical power networks. This concept paves the way for future work on grid services provided by prosumers. For instance, DERs would assume P2P power supply responsibility for the reliability of the electricity to customers they trade with. Both DERs and consumers are incentivized to actively participate in trading, with improved benefits from the P2P market designed in this paper.

3.4. Robustness check for the loss function and the coefficient alpha

The proposed model integrates technical and economic aspects, interlacing network physical analysis with variable outputs from DERs. This holistic perspective necessitates accuracy and robustness in every component of the model. The loss function directly affects the calculation of network losses, a key constraint that shapes the viable physical supply of electricity and asset usage. On the other hand, the coefficient α determines the cost allocation strategy in the trading model. It plays a critical role in striking a balance between the incentive for DERs to increase their outputs and ensuring a reasonable cost for consumers. Given these central roles, any sensitivity or variance in these two parameters could have far-reaching implications on the overall performance and validity of the market architecture. Hence, it is crucial to investigate their robustness thoroughly, to ensure that findings are not only theoretically sound, but also practically applicable in optimizing

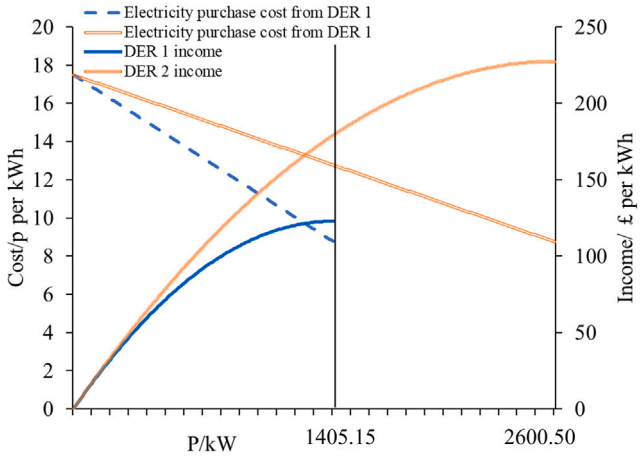

Fig. 5. Costs and total income functions of DER 1 and DER 2.

transaction costs and maximizing benefits for all participants in the P2P electricity market.

A robustness check of the loss function was conducted. This check involved evaluating the loss function using alternative settings to test the impact of different functional forms on the model's outcomes. The original form of our loss function is defined as $f^{loss}(x) = m \cdot ln(x) + ax^2 + bx + c$.

Three distinct loss functions were evaluated during the robustness checks. Function I, defined as $f^{loss}(x) = m \cdot ln(x)$, was assessed to measure the effect of logarithmic scaling on the ratio of DER active power output to the total network load. Function II, which is a quadratic polynomial expressed as $f^{loss}(x) = ax^2 + bx + c$, was analyzed to understand the impact of quadratic relationships among the variables. Finally, Function III, a higher-order polynomial given as $f^{loss}(x) = d \cdot x^3 + ax^2 + bx + c$, was explored to ascertain the model's sensitivity to cubic terms that can encapsulate complex, nonlinear relationships, potentially improving model accuracy.

The robustness check for the loss function highlights the importance of the choice of function form on loss allocation calculations, and consequently, on the distribution of active DER power output. As illustrated in Table 7, we utilize the loss indexes of DER 2 in DER 1's upstream market as test cases for verification. The outcomes of these robustness evaluations provide substantial insights and will be detailed in the forthcoming sections. Notably, the original function offered a balanced depiction of the inherent dynamics, while maintaining an acceptable error range of 4.10×10^{-4}. This level of precision is not equally maintained in the alternative models, with Function I, Function II, and Function III exhibiting standard errors of 5.63×10^{-1}, 2.64×10^{-3}, and 1.38×10^{-3} respectively.

In delving into the specifics of the function forms, the original function, provides a unique perspective. The parameters a, b, and c define the quadratic polynomial component and have estimated values of −0.0492, 0.0800, and 0.8813 respectively. The weight of the natural logarithmic term, represented by parameter m is −0.0464. The balanced weights of these parameters manifest in the curve's shape and position, which closely mirrors the observed data. In contrast, Function III, carries a much smaller weight of the x^3 term (parameter $d = 0.0117$). Coupled with the lower weights of the quadratic and linear terms ($a = 0.0190$, $b = 0.0092$), the higher standard error (0.0013) suggests a less accurate depiction of the underlying phenomena. Ultimately, the balanced weights of the parameters in the original function offer a more accurate and robust representation of the observed data.

In assessing the robustness of α, we conducted an extensive exploration on the influence of equidistant sampling within the range of $(0, 1.0]$. This model, defined by electricity purchase cost from DER i as shown in Eq. (9), is dependent on α for calculating the electricity purchase cost and subsequently the income derived from DERs.

When $\alpha < 0.5$, the discount the customer receives is relatively small. As a result, the cost the customer pays to DER i is higher. While this could be seen as advantageous for the DER as it receives higher income per unit hence willing to have maximum output, as shown in Fig. 6(a) and (b). However, when α is close to 0, it means that the discount the customers receive is negligible. In other words, the per-unit cost that customers have to pay for energy from the DER, $Cost_i^{DER}$, is nearly the same as the cost of energy from the grid, $Cost^{Grid}$. From the customers' perspective, this might not provide much incentive to buy energy from the DER, as the cost is almost the same as the grid price but potentially with added complexities or uncertainties related to DER supply. This lack of incentive might reduce the demand for energy from local DERs.

When $\alpha > 0.5$, the discount customers receive on the energy cost becomes more significant, thereby reducing the per-unit cost $Cost_i^{DER}$ that customers have to pay for energy from the DER. This might be attractive for customers as they get to pay less for their energy needs compared to the grid price. However, from the DER's perspective, a larger α implies that the income per unit energy sold decreases, since customers are now buying energy at a lower cost. This could potentially lead to discouraging DERs, such as wind or solar energy sources, to maximize their outputs. In the assessment of DER outputs with varying α values, it is observed that the DER 1 output does not reach the maximum potential of 1405.15 kW for α values beyond 0.5. Specifically, when α equals 0.6, the DER output is approximately 1170.96 kW, which decreases to 1003.68 kW, 878.22 kW, 780.64 kW, and 702.57 kW for α values of 0.7, 0.8, 0.9, and 1.0, respectively. Similarly, as α increases from 0.6 to 1.0, the DER 2 output decreases significantly from 2167.1 kW to 1857.5 kW, 1625.3 kW, 1444.7 kW, and finally 1300.3 kW which cannot reach the maximum potential of 2600.50 kW. When α equals 1, it implies that the energy from the DER is free when DERs reach the maximum output, which is unrealistic, as shown in Fig. 6(c) and (d).

When $\alpha = 0.5$, a balance point is achieved by ensuring that both DERs are incentivized to produce up to their maximum capacity, and customers are not burdened with high energy costs. At this level, the cost per unit of DERs is reasonable enough to motivate DERs to reach their maximum output of 1405.15 kW and 2600.50 kW separately, resulting in their income reaching the maximum. Meanwhile, the cost to the consumer remains at a fair rate, preserving the demand for DER-produced energy. Our data analysis indicates that an α of 0.5 appears to be a good compromise that takes into account both DERs' and consumers' perspectives, while ensuring model realism and robustness.

4. Conclusion

This paper reports work on building a new P2P energy market model supported by dynamic power flow tracing in power distribution networks. An optimized market segmenting strategy based on identifying power transactions is proposed. Graph-based modeling is applied to determine electricity transaction costs and maximize the benefits of both DERs and consumers by quantifying each transaction's usage of the network with allocated losses.

The key findings of the proposed work can be summarized as follows: The proposed model effectively/successfully established a promising link between the P2P energy market and distribution network infrastructure from generation to consumption by considering the technical constraints. The introduced market segmentation approach based on transaction-oriented dynamic power flow tracing can technically and economically define the market boundaries in a physical system. The optimization results of the proposed model demonstrated opportunities for profits within several markets segmented by power flow tracing, compared with the existing centralized market with unified incentives for both individual DER owners and consumers. It showed a high potential to increase the DER owners' revenue that varied between

Table 7
Robustness check for the loss function based on loss indexes of DER 2 in DER 1 upstream market.

	m	*d*	*a*	*b*	*c*	Error[a]
Original form	−0.0464	–	−0.0492	0.0800	0.8813	4.10E−04
Function I	−0.7859	–	–	–	–	5.63E−01
Function II	–	–	0.0701	−0.1517	0.9992	2.64E−03
Function III	–	0.0117	0.0190	0.0092	0.0013	1.38E−03

[a] Standard error of the regression.

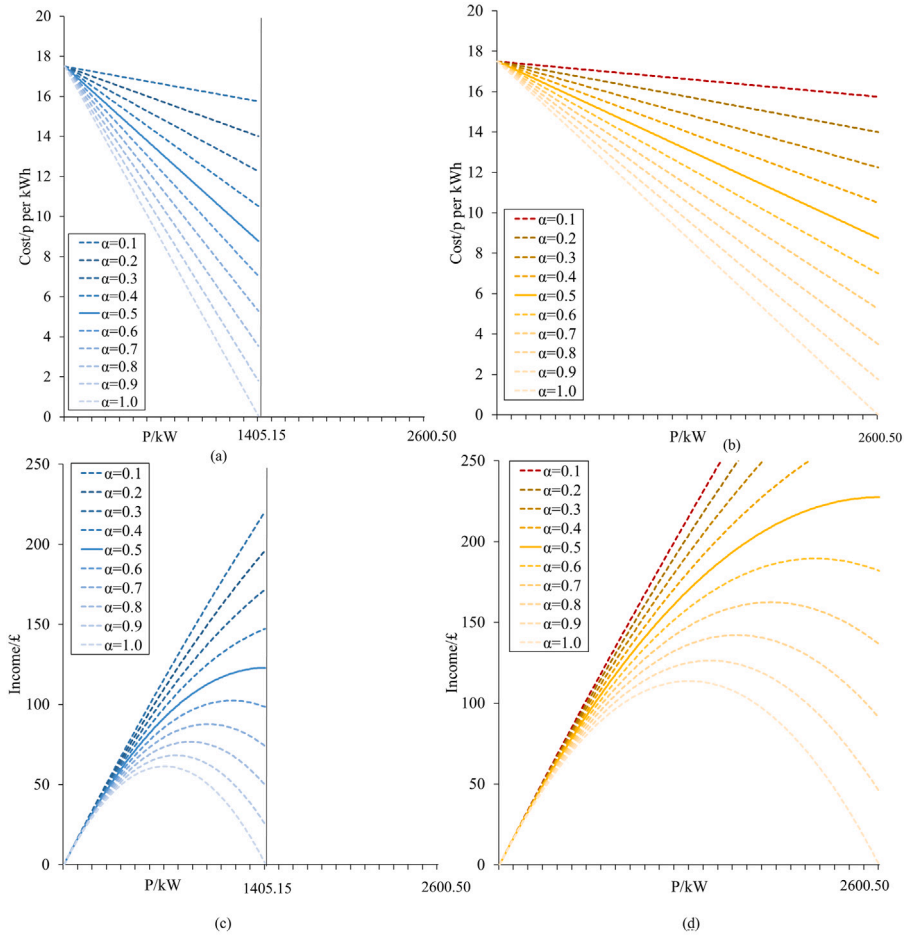

Fig. 6. Robustness check for α of (a) Electricity purchase cost from DER 1 (b) Electricity purchase cost from DER 2 (c) DER 1 Income (d) DER 2 income.

£1264.58 and £1910.79; when compared with a traditional FiT model; meanwhile, consumers see reduced bills of up to £1736.44 (as shown in the Case Study) with lower tariffs.

The proposed P2P electricity market encourages DERs to operate at their maximum/rated capacity with high profit. Meantime, more contributing and sharing of DERs in the network are related to more power losses they take responsibility for. It also reveals that DERs located close to the tails of the network have a higher market proportion than DERs locate close to the substation. This could encourage installations of DERs towards the end of the networks helpful to alleviate potential voltage drop issues. For potential over-voltage issues, optimally controllable DERs can reduce their net output to overcome voltage rise constraints (e.g. curtailing by limiting maximum power point tracking, or combining battery energy storage systems). It is anticipated that higher-cost DERs could be firstly cut, but they would be able to change bidding strategy to avoid that, based on their own profit optimization. Meanwhile, the robustness checks clearly illustrate the critical impact of both the loss function and the coefficient alpha on the DER costs and income, signifying their essential roles in maximizing DER output and optimizing customer costs, underscoring the importance of prudent parameter selection and model formulation in energy market studies.

The network usage charges of all transactions and pricing strategies of DERs would require further research, taking into account the life of equipment/assets, such as transformers, switches and wires, and DERs' capital investment. Meanwhile, stochastic optimization needs to be further considered with solar panels and wind turbines' power output depending on the weather.

CRediT authorship contribution statement

Chengwei Lou: Conceptualization, Methodology, Implementation, Writing – original draft. **Jin Yang:** Conceptualization, Methodology, Writing – original draft editing. **Eduardo Vega Fuentes:** Visualization, Investigation. **Yue Zhou:** Methodology, Reviewing, Editing. **Liang Min:** Software, Validation. **James Yu:** Supervision, Reviewing. **Nand Kishor Meena:** Reviewing and editing.

Declaration of competing interest

The authors declare that they have no known competing financial interests or personal relationships that could have appeared to influence the work reported in this paper.

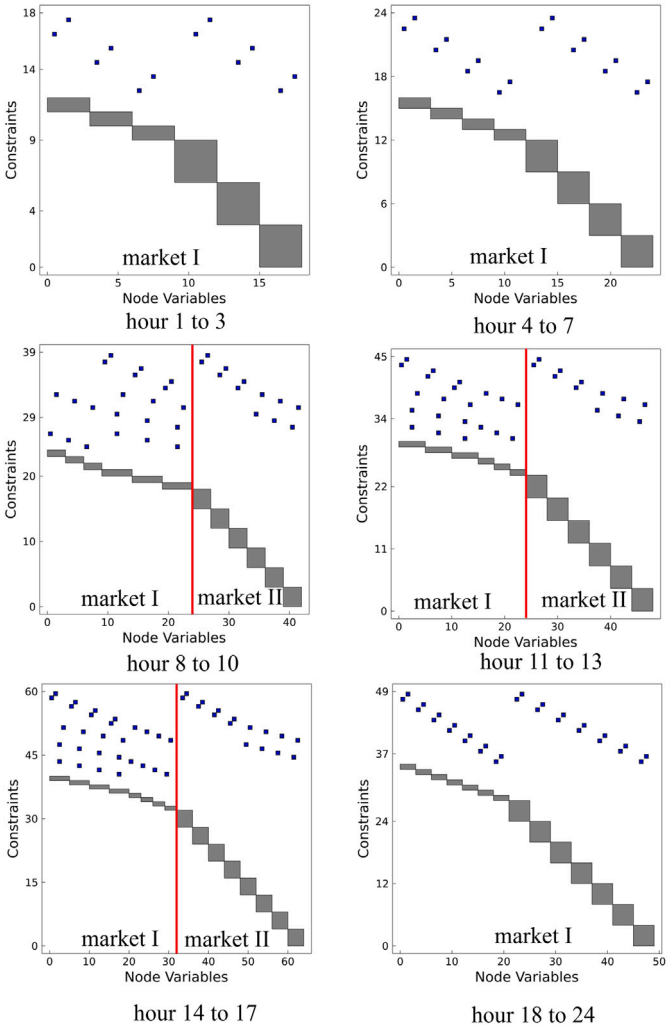

Fig. 7. Graph matrix of 24-h market.

Data availability

Relevant data have been referred to the original sources.

Acknowledgments

The work is supported by the Engineering and Physical Sciences Research Council (EPSRC, United Kingdom) in project "Street2Grid – an electricity blockchain platform for P2P energy trading" (Reference: EP/S001778/2).

Appendix

The graph matrix generated for the case study is shown in the Fig. 7, with blocks representing OptiNode and blue marks representing linking constraints that connect their variables [35]. Blocks' number in one graph equal to hours × participants' number. For example, hours 1 to 3 have two participants. Therefore, there are 6 blocks.

In hours 8 to 10, hours 11 to 13 and hours 14 to 17, market I has more blue marks than market II. This is due to that market I has three participants, DER 1, DER 2 and $load_a$; conversely, market II have two participants DER 2 and $load_a$. The number of the link constraints between three participants is more than the that of the link constraints between two participants.

References

[1] Foxon TJ. Transition pathways for a UK low carbon electricity future. Energy Policy 2013;52:10–24.
[2] Department for Business, Energy & Industrial Strategy. The ten point plan for a green industrial revolution. Technical report, Prime Minister's Office, 10 Downing Street, The Rt Hon Alok Sharma MP, and The Rt Hon Boris Johnson MP; 2020.
[3] John JS. How the UK Is Building Grid Markets to Reward Flexible Distributed Energy. 2020, https://www.greentechmedia.com/articles/read/how-the-uk-is-building-grid-markets-to-reward-flexible-distributed-energy.
[4] Tushar W, Saha TK, Yuen C, Morstyn T, Poor HV, Bean R, et al. Grid influenced peer-to-peer energy trading. IEEE Trans Smart Grid 2019;11(2):1407–18.
[5] Smith P, Beaumont L, Bernacchi CJ, Byrne M, Cheung W, Conant RT, Cotrufo F, Feng X, Janssens I, Jones H, et al. Essential outcomes for COP26. Glob Change Biol 2021.
[6] Ye L-C, Rodrigues JF, Lin HX. Analysis of feed-in tariff policies for solar photovoltaic in China 2011–2016. Appl Energy 2017;203:496–505.
[7] Cherrington R, Goodship V, Longfield A, Kirwan K. The feed-in tariff in the UK: A case study focus on domestic photovoltaic systems. Renew Energy 2013;50:421–6.
[8] Ofgem. Scheme tariff tables. 2021.
[9] British Gas. Our tariffs. 2021, http://www.britishgas.co.uk, Accessed: 2021-12-05.
[10] Ofgem. About the smart export guarantee (SEG). 2021, https://www.ofgem.gov.uk/environmental-programmes/smart-export-guarantee-seg/about-smart-export-guarantee-seg, Accessed: 2021-12-05.
[11] Vega-Fuentes E, Yang J, Lou C, Meena NK. Transaction-oriented dynamic power flow tracing for distribution networks—Definition and implementation in GIS environment. IEEE Trans Smart Grid 2021;12(2):1303–13.
[12] Parag Y, Sovacool BK. Electricity market design for the prosumer era. Nat Energy 2016;1(4):1–6.
[13] Cui S, Wang Y-W, Shi Y, Xiao J-W. Community energy cooperation with the presence of cheating behaviors. IEEE Trans Smart Grid 2021;12(1):561–73.
[14] Cui S, Wang Y-W, Shi Y, Xiao J-W. A new and fair peer-to-peer energy sharing framework for energy buildings. IEEE Trans Smart Grid 2020;11(5):3817–26.
[15] Cui S, Wang Y-W, Xiao J-W. Peer-to-peer energy sharing among smart energy buildings by distributed transaction. IEEE Trans Smart Grid 2019;10(6):6491–501.
[16] Cui S, Wang Y-W, Xiao J-W, Liu N. A two-stage robust energy sharing management for prosumer microgrid. IEEE Trans Ind Inf 2019;15(5):2741–52.
[17] Morstyn T, Teytelboym A, Mcculloch MD. Bilateral contract networks for peer-to-peer energy trading. IEEE Trans Smart Grid 2019;10(2):2026–35.
[18] Hug G, Kar S, Wu C. Consensus + innovations approach for distributed multiagent coordination in a microgrid. IEEE Trans Smart Grid 2015;6(4):1893–903.
[19] Sorin E, Bobo L, Pinson P. Consensus-based approach to peer-to-peer electricity markets with product differentiation. IEEE Trans Power Syst 2019;34(2):994–1004.
[20] Cui S, Wang Y-W, Li C, Xiao J-W. Prosumer community: A risk aversion energy sharing model. IEEE Trans Sustain Energy 2020;11(2):828–38.
[21] Cui S, Wang Y-W, Shi Y, Xiao J-W. An efficient peer-to-peer energy-sharing framework for numerous community prosumers. IEEE Trans Ind Inf 2020;16(12):7402–12.
[22] Liu N, et al. Online energy sharing for nanogrid clusters: A Lyapunov optimization approach. IEEE Trans Smart Grid 2018;9(5):4624–36.
[23] Tushar W, Saha TK, Yuen C, Smith D, Poor HV. Peer-to-peer trading in electricity networks: An overview. IEEE Trans Smart Grid 2020;11(4):3185–200.
[24] Usman M, Coppo M, Bignucolo F, Turri R, Cerretti A. Multi-phase losses allocation method for active distribution networks based on branch current decomposition. IEEE Trans Power Syst 2019;34(5):3605–15.
[25] Guerrero J, Chapman AC, Verbič G. Decentralized P2P energy trading under network constraints in a low-voltage network. IEEE Trans Smart Grid 2018;10(5):5163–73.
[26] Costa P, Matos M. Loss allocation in distribution networks with embedded generation. IEEE Trans Power Syst 2004;19(1):384–9.
[27] Savier JS, Das D. Impact of network reconfiguration on loss allocation of radial distribution systems. IEEE Trans Power Deliv 2007;22(4):2473–80.
[28] Mutale J, Strbac G, Curcic S, Jenkins N. Allocation of losses in distribution systems with embedded generation. IEE Proc, Gener Transm Distrib 2000;147(1):7–14.
[29] Kumar P, Gupta N, Niazi KR, Swarnkar A. A circuit theory-based loss allocation method for active distribution systems. IEEE Trans Smart Grid 2019;10(1):1005–12.
[30] Carpaneto E, Chicco G, Akilimali J. Branch current decomposition method for loss allocation in radial distribution systems with distributed generation. IEEE Trans Power Syst 2006;21(3):1170–9.
[31] Abdelkader SM. Transmission loss allocation through complex power flow tracing. IEEE Trans Power Syst 2007;22(4):2240–8.

[32] Keay M. The EU "Target Model" for electricity markets: fit for purpose. Oxford Inst Energy Stud 2013.
[33] Boyd SP, Vandenberghe L. Convex optimization. Cambridge University Press; 2004.
[34] McCloskey DN, Ziliak ST. The standard error of regressions. J Econ Lit 1996;34(1):97–114.
[35] Jalving J, Shin S, Zavala VM. A graph-based modeling abstraction for optimization: Concepts and implementation in Plasmo.jl. 2020.
[36] Bezanson J, Edelman A, Karpinski S, Shah VB. Julia: A fresh approach to numerical computing. SIAM Rev 2017;59(1):65–98.
[37] Dunning I, Huchette J, Lubin M. JuMP: A modeling language for mathematical optimization. SIAM Rev 2017;59(2):295–320.
[38] Thurner L, Scheidler A, Schäfer F, Menke J-H, Dollichon J, Meier F, Meinecke S, Braun M. Pandapower—An open-source python tool for convenient modeling, analysis, and optimization of electric power systems. IEEE Trans Power Syst 2018;33(6):6510–21.
[39] Virtanen P, et al. SciPy 1.0: fundamental algorithms for scientific computing in Python. Nat Methods 2020;17(3):261–72.
[40] British gas: Our tariffs. 2020, http://www.britishgas.co.uk, Accessed: Jul. 15, 2020.